Library Progress International *Print version ISSN 0970 1052*
Vol.44 No. 3, Jul-Dec 2024: P.10723-10734 *Online version ISSN 2320 317X*

Original Article *Available online at www.bpasjournals.com*

Improved Emotion Identification with Novel Feature Extraction Technique Utilizing EEG Data

Kirti[1], *Yogendra Narayan[2], Rajeev Ranjan [3]

[1]Department of Electronics and Communication Engineering
Chandigarh University Mohali, India
hooda.kirti04@gmail.com
[2]Department of Electronics and Communication Engineering
Chandigarh University Mohali, India
narayan.yogendra1986@gmail.com
[3]Department of Electronics and Communication Engineering
Chandigarh University Mohali, India
rajeevranjan1134@gmail.com

How to cite this article: Kirti, Yogendra Narayan, Rajeev Ranjan (2024). Improved Emotion Identification with Novel Feature Extraction Technique Utilizing EEG Data. *Library Progress International*, 44(3), 10723-10734.

ABSTRACT
In the recent era of technology, Automatic emotion detection has become a versatile tool due to the significance application of emotions recognisition. With the increasing popularity of human-computer interface applications, this study focuses on the identification of emotions using electro-encephalography (EEG) signals. The proposed approach offers a method to recognize the basic emotions using advance machine learning method. The aim of this research is to build an intelligent strategy that uses discrete signal processing for improving the accuracy of emotion identification by employing Support Vector Machines (SVM). The results show that the accuracy of proposed approach was found 98.23% for identifying the four different emotions like happiness, sad, current, and hate.

Keywords: S-Transformation, Emotion recognition, emotion model, SVM, EEG, NN.

1. Introduction

Imagine the human brain as an electronic computer that converts sensory data (sensory information) into electrical data (voltage) (electroencephalogram, or EEG). This process is known as electrochemistry. Emotions are intricate instructions that correspond to physiological changes in the human body. Emotions such as sadness, anger, hatred, hope, despair, fear, melancholy, happiness, surprise and others can be utilized to create an emotion recognition system. A wide range of disciplinary fields in psychology and engineering have expressed a great deal of interest in last decade years in research on emotion identification based on electroencephalography (EEG), including advanced approach on emotion theory and application to afficient brain-computer interfacing (BCI) [1]. This advance BCI systems by making it possible to recognize, interpret, and react to emotive experiences through physiological signals.

An individual's brain signals are significantly impacted by the fluctuations in their emotions. Consequently, there has been a surge in demand for EEG, which capture electrical information from the brain, in recent years. The electrodes used in EEG recording systems capture 3 to 256 relative voltages on the scalp, depending on the use case. Typically, 8 to 32 ECG channels are required for clinical applications. This work can elicit different emotions in others by using photos, films, writings, and music [2]. As a result, this work can capture the emotional signals. The recognition algorithms then make use of the recorded signals, sometimes referred to as the database. Various categorization methods and extracted characteristics serve as the foundation for different diagnostic processes. For instance, the quantity and kind of channels in an ECG signal might be regarded as identifying parameters. AMIGOS Performance, Wavelet Scattering Feature Extraction and Supervised Machine Learning, and Russell's Circumflex Emotion Recognition Algorithm. This is a dataset for individual research on mood, personality, and effects [3]. Figure 1 show the two-dimensional distribution of emotions. Valence is represented on x-axis and arousal on y-axis.

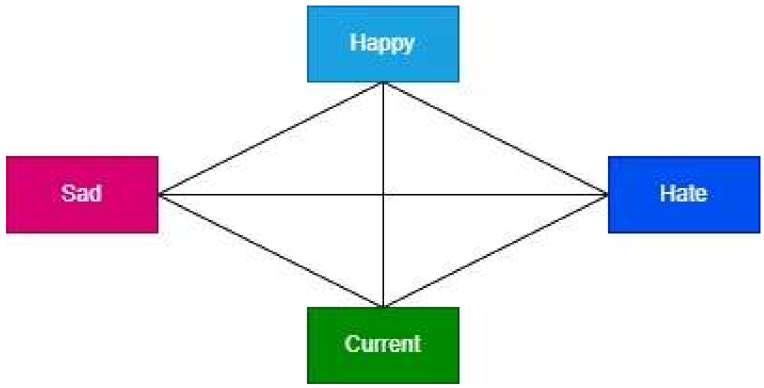

Figure 1: Valence Arousal Model

An EEG signal has a wealth of information that may be retrieved. The EEG signal may be altered in several ways to produce these properties. The Fourier transform, for example, focuses on a certain frequency range. The classification job employs a non-linear approach to set the boundaries of the judgments. There have been several published classification techniques for using an EEG signal to identify emotions. These approaches, which are listed as the most often used ones, include self-validation (SVM), k-nearest neighbors (KNN), NN classifier [4].

Typically, the emotions under study can be classified as either good, negative, or neutral. While persistently negative emotions can be detrimental to people's health, well-being, and career opportunities, positive emotions can increase emotional and subjective well-being. Compared to other emotions, neutral sentiments are rather bland and lack either a pronounced pleasure or misery [5]. In essence, fine-grained emotion detection makes it possible to determine an emotion's intensity. Because machine learning and deep learning methods have shown to be an effective means of handling the laborious pre-processing and feature extraction procedures involved in multimodal emotion recognition, they are the main focus of this work. They outperform traditional techniques in terms of classification and have higher accuracy when it comes to emotion detection. New technical methods like artificial intelligence, federated learning, and transfer learning can be utilized to assess human emotion states [6].

Here's what's left in this section: the background is given in Section 2. The proposed work methodology has included in Section 3. The experimental data and contrast our emotion recognition model with various approaches in Section 4. The assessment of proposed emotion identification system using the DEAP dataset is given in the Section 5.

2. Background

A computer-implemented job that has been researched extensively is emotion recognition. Video records, voice recordings, and facial and body scans are the most often used inputs for emotion identification. Emotion recognition tasks on annotated data sets have been performed by machine learning (ML) algorithms in recent years. Zhong. et al. [7] proposed a Deep-Emotion, a deep learning-based “Multimodal Emotion Recognition (MER)” system that may be used to enhance MER performance by adaptively integrating the most distinguishing characteristics from speech, facial expressions, and “Electroencephalograms (EEG)”. Abdullah A. et al. [8] used mixed text, audio (voice), and visual data modalities using features from independently pre-trained self-supervised learning models. The most significant obstacle in multimodal emotion categorization research is the integration of features and representation.

Sharma Z et al [9]. have discussed the novel transformer and attention-based fusion strategy is presented, which incorporates multimodal autonomous learning characteristics and yields 86.40% accurate multimodal results for emotional categorization. The "discriminatively deep fusion" technique utilizing an im-conditioned generic adversarial network (IM-cGAN) has achieved 94.23% data accuracy. Use the D-loss function to increase the inter-class variances and decrease the intra-class distances to obtain a fused feature representation that will enhance the fused features' discrimination. Use both local features from the region-based module and global features from the global-based module.

Liu S. et al. [10] provide a two-stage "Hybrid Deep Feature Selection (HDFS)" system that excels in accuracy and computational efficiency for recognizing emotions from human voices by fusing automated feature engineering with deep learning. A 5-fold cross-validation technique is utilized for assessing the suggested pipeline on three SER datasets that are made available to the public. Iyer A. et al. [11] suggest a double-way deep residual NN that uses brain network analysis in conjunction with it to classify different emotional states. Eight volunteers participated in a series of studies conducted by the author to obtain their emotional EEG. Using our emotional dataset, the suggested model's average accuracy is 94.57%.

Prakash PR. et al. [12] focus on applying techniques for EEG source imaging (ESI) to extract active emotional cortical sources. Participants' emotions are quickly and effectively induced through auditory stimuli. The "EEG Source-based GNN node (ESB-G3N)" algorithm uses active EEG sources as graph nodes. In comparison to subject-dependent and subject-independent scenarios, the results demonstrate an absolute improvement of 1-2 percent. Sarvakar K. et al. [13] focus on applying techniques for EEG source imaging (ESI) to extract active emotional cortical sources. Participants' emotions are quickly and effectively induced through auditory stimuli. The "EEG Source-based GNN node (ESB-G3N)" algorithm uses active EEG sources as graph nodes. In comparison to subject-dependent and subject-independent scenarios, the finding demonstrate an absolute improvement of 1-2 percent.

Chowdary MK. et al. [14] have proposed a novel spatial system of multi-channel EEG signals, known as a hybrid convolutional recurrent NN (HCRNN). The "Tunable Q-factor Wavelet Transform (TQWT)" feature extraction method is part of the innovative EEG-based emotion identification system that is proposed. To break down the EEG into multiple sub-bands with stationary properties, TQWT is initially used based on the oscillation behavior of the signals. Ramzan M. et al. [15] provide an overview of deep learning-based emotional identification of multimodal inputs and compare its applications based on ongoing research. Because multidimensional affective computing (MECs) have a greater classification accuracy than multimodal ones, they are explored in conjunction with multimodal affective computing.

3. Materials and Methods

The objective of the approaches described is to provide a workable approach for identifying appropriate features and classifiers. The goal of this research is to improve the ability to recognize emotions from brain signals by concentrating on both feature extraction and classifier. Counting the number of EEG channels that will be utilized for the feature extraction process is the first stage. After that, the database signals will be subjected to the feature extraction process. Lastly, a classification of the retrieved characteristics and an assessment of the suggested method's efficacy will be conducted.

3.1 Database

The suggested approach is initially evaluated using the DEAP dataset, a comparative multimodal dataset. The EOG signals of 32 individuals were recorded while they watched 40 various kinds of music videos to create this dataset (see Fig. 1). The participants were in good health, with ages ranging from 19 to 32, and 50% of them were female. Affective tags were utilized to group the music videos that were used as stimuli into distinct emotional categories. Each movie was scored by the participants according to its arousal, valence, likeness, dislikeness, dominance, and familiarity. Before being used, the EEG of the subjects were captured at a rate of 128 Hz. Please take notice that the data may be downloaded from EECS.IQMUL.COM /MMV / Datasets / Deap in MATLAB format [16].

3.2 Channel selection methodology

The dataset utilized to evaluate the suggested method consists of 32 channels of data that can be processed in 63 seconds at a frequency of 128 Hz for each individual, as stated in Subsection 3.2. As such, each individual has a substantial amount of data that has to be processed. There are two issues with this, though: first, processing takes a long time, and second, a lot of storage memory is needed to hold all of the data. These two disadvantages led us to reduce the data set, without sacrificing classification accuracy. This work discovered those 7.5 seconds of data from the research are appropriate for our suggested algorithm's easy feature extraction [17].

This significantly lowers. The number of channels and feature extraction time should be minimized if the technique is intended for real-time application. The comfort of the user when using the device may also be impacted by the usage of many electrodes. As a result, our primary objective is to create an algorithm that operates in real-time with adequate precision [18]. The most effective routes have been found using a variety of methods, mainly including heuristic optimization algorithms or trial-and-error [19], [20], [21], [22], and [23]. Based on the outcomes of these techniques, this work compares two sets of channels in this study. Three channels (P7, P3, and PZ) make up one group; seven channels (C4/CP2//O1/ PO3/ PZ/ P3/ P7) make up the other.

3.3 Feature Selection: Proposed Methodology

The two stages of the suggested feature extraction approach are separated. First, the EEG signal is split into fundamental frequency bands using the S-Transform. Second, the Gabor Wavelet feature and the intrinsic mode functions feature are employed. Lastly, the effective frequency band of the data is determined using the S-Transform's PE values. The last step is to break down the obtained EEG data using the S-Transform [24].

3.3.1 Decomposition of EEG signal using S-Transformation

Conversely, the S-Transform is a CWT variation that is built around an expanding and moving Gaussian window are given in Figure 2. Proposed Methodology for Optimal EEG Frequency Band Selectivity: Evolution from CWT.

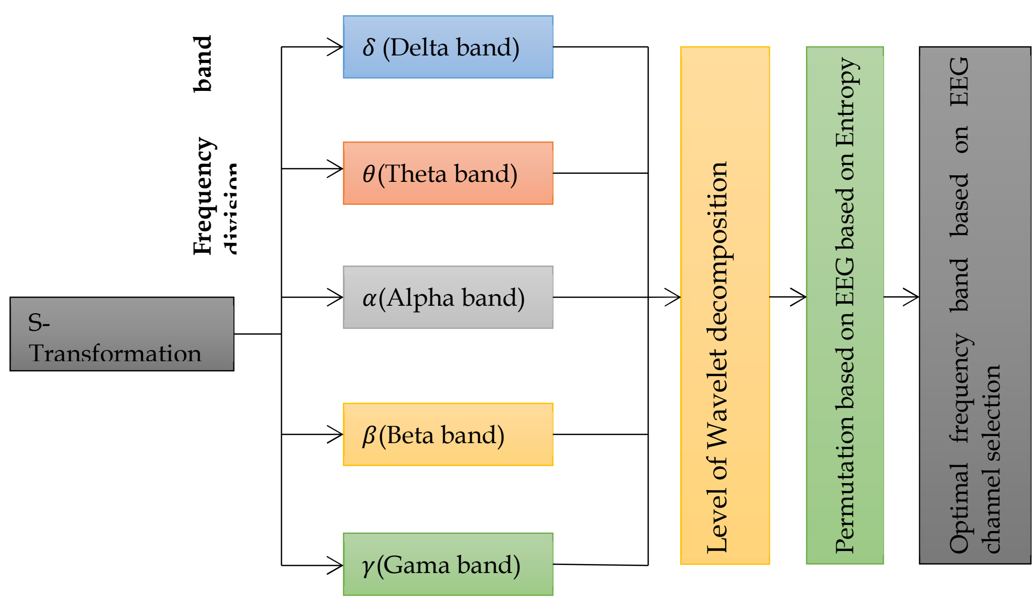

Figure 2: Methodology proposed for EEG frequency band selection

Equation 1 defines the Conveyance Weighted Wavelet (CWT) of the $g(t)$ signal with a certain mother wavelet given in equation 1.

$$\omega(\tau,d) = \int_{-\infty}^{\infty} g(t)\omega(\tau - t)dt$$

(1)

where d stand for dilation parameter; t is the time; τ stand for spectral localization time; w is the mother wavelet as given in the equation 2

$$S(\tau,f) = e^{j2\pi f\tau} W(\tau,d) \quad (2)$$

The mother wavelet w is chosen to be positive and Gaussian, i.e.

$$w(\tau,f) = \frac{|f|}{\sqrt{2\pi}} e^{\frac{-t^2 f^2}{2}} e^{-i2\pi f}$$

(3)

The inverse frequency of the dilation parameter in this instance is represented by d. Given that the allowable wavelet in Equation (4) has a zero mean, the S-transform is expressed as

$$s(\tau,f) = \frac{|f|}{\sqrt{2\pi}} \int_{-\infty}^{\infty} g(t) e^{\frac{-t^2 f^2}{2}} e^{-j2\pi f t}\,\mathrm{dt}$$

(4)

$$s(\tau,f) = \int_{-\infty}^{\infty} g(t)\omega(\tau - t, f) e^{-j2\pi f t}\mathrm{dt}$$

(5)

where f is the signal's frequency. The Fourier transform of the signal yields the discrete transformation of the signal. Let the discrete time series of the continuous-time signal, $g(t)$, be represented as $[kT\ ]$, $k = 0,1,\dots,N$. The time signal's sampling interval is determined in Equation 6.

$$G\left(\frac{n}{NT}\right) = \frac{1}{N}\sum_{K=0}^{N-1} g(kT) e^{\frac{-i2\pi f t}{N}} \qquad n = 0,1, \dots \dots \dots n-1$$

(6)

In the discrete instance, the S-transformation is the transformation of a vector on a spanning collection of vectors (FTs) specified by a time series ($g[kT\ ]$). A Gaussian element product with an i-shifted Gaussian divides each FT basis vector into n localized vectors, and the total of the N localized vectors equals the original basis vector. Refer to Eq.7 for discrete time series.

$$S\left(\frac{n}{N+1}, jT\right) = \sum_{m=1}^{N-1} G\left(\frac{m+n}{NT}\right) H(n.m) e^{\frac{i2\pi m j}{M}} \quad (7)$$

with $j, m, n = 0,1,\dots,N-1$ and $H(n.m)e^{\frac{i2\pi mj}{M}}$, and formula (7): S-matrix: The N × M matrix is called the S-matrix. The frequency is represented by the rows and the time by the columns of the S-matrix. Function of the Gaussian window: This work examines the Gaussian window function to S-transformation time series data in this paper. Time-frequency diagram: The dynamics of time-frequency signals are frequently studied using non-stationary signals. The Gabor transform, the Church-Corte transform (Corte-Corte), the Short Time Fourier transform (STFT), and a bilinear class called Cohen's class are often used as time-frequency representations. STFT's limitations include restricted time resolution for high frequencies and reduced frequency resolution for low frequencies due to its set-sized window length.

The window function is a function of frequency and time in the S-Transform as given in Eq. 3. As a result, for low frequencies, For higher frequencies, the S-Transform offers strong temporal localization as well as good frequency localization. The S-Transform maintains a direct relationship with the FFT while offering strong frequency-dependent resolution since it accepts frequency as a parameter. As demonstrated by CWT, this S-Transform characteristic enables the representation of the signal in the temporal plane as opposed to the time-scale plane.

Time-frequency representation (TFP) is a useful tool for analyzing the dynamics of non-stationary signals. The bilinear group of temporal frequency distributions (Cohen's class), CWT (Consequential CWT), STFT, and Gabor transform (GFT) are often utilized TFPs in this application. Every TFP, though, has its limitations. For instance, STFT has poor frequency resolution for low frequencies and restricted temporal resolution for high frequencies due to its fixed-sized window length. This indicates that the S-Transform can offer good localization for higher frequencies in the time domain and low frequencies in the frequency domain.

While S-transform retains a direct link with FT, it gives a high resolution that is reliant on frequency since it accepts frequency as a parameter. As opposed to the time scale plane used in CWT, this S-transform feature enables signal representation on the time-frequency plane. In contrast to CWT, which just localizes the signal's amplitude, whereas the S-Transform maintain both amplitude as well as phase information. Because S-Transform has benefits over STFT and CWT, this work concentrated on improving EOG channels and extracting characteristics to identify alertness level detection. The three-dimensional S-transform coefficients of six subjects in both awaking and sleep situations against the frequency as well as time axes. The optimal channels can be found in several ways, usually involving trial and error or the application of heuristic optimization algorithms. This study compares two sets of channels using the outcomes of these methodologies. Three channels, δ (Delta band), θ(Theta band), and α(Alpha band) make up the first group. The remaining channels as alpha and beta in the second group. There are very few channels as a result.

3.3.2 Gabor feature extraction

It has been shown that Gabor filters also referred to as Gabor wavelets or kernels are an effective technique for extracting features. Band-limited filters with ideal spatial and frequency localization are referred to as Gabor filters [38].

$$\varphi(x,y) = \frac{fu^2}{\pi\gamma\mu} exp\left(-\left(\frac{f^2}{\gamma^2}x^2 + \frac{f^2}{\mu^2}y'^2\right)\right) \exp\left(j^2\pi fux'\right)$$

(8)

where $x' = x\cos\theta + y\sin\theta_2$, $y' = -x\sin\theta_v + y\cos\theta_v$ $f_u = \frac{f_{max}}{2^{u/2}}$ and $\theta_v = v\frac{\pi}{8}$

Every filter functions as a Gabor kernel function, modulated by complex plane waves, whose corresponding orientation (R-1) and center frequency (CF) are determined by f_u and θ_v. When set to a constant value, the γ parameter guarantees that a Gabor filter with varying scales and orientations behaves similarly to scaled copies of itself. It establishes the ratio between the center frequency and the size of the Gaussian envelope. It is essential to remember that the center frequency (F) of the filter (R-1) uniquely defines the Gabor filter scale, given a constant value of γ and scale. The γ parameter's value of 0.25 guarantees that the Gabor filter banks (√2). Usually, the last parameter f_{max} is f = f.25. The maximum frequency of the filter is represented by this parameter. Four or five scales and six or eight orientations of Gabor filter banks are used by most studies [39]. The simulation of Gabor wavelets involves two steps, the first is Build Gabor filters with the aid of a mathematical formula and another is Convolution through a two-dimensional matrix of the filters.

The data of each channel chosen in each row is used to create the matrix that has to be convolved with the Gabor filter bank in this work. The next stage after convolution is to extract relevant features from the created matrices. Three characteristics are examined in this paper: OGGP (Optimized Gabor phase Congruency Pattern), energy, and mean amplitude. The two-dimensional matrices that correspond to the number of Gabor filters as outputs are the energy convolution of the Gabor filters and the formation of a two-dimensional matrix. The energy must be computed using a 2D Fourier transform for each output matrix. For example, 40 Gabor filters with the EEG data after counting them by 5 scales with 8 distinct orientations.

Consequently, this work has created 40 matrices and utilized their energies as characteristics. The mean amplitude is the second characteristic. The average of the output matrix element's total area is used to compute the mean amplitude. The Oriented OOGPCP pattern is the third characteristic. Even if the picture sites are sampled a few pixels apart, the Gabor phase contains as known highly diverse values, while the Gabor magnitude fluctuates slowly with spatial position. As a result, extracting trustworthy and differentiable information from phase responses is challenging. This is because the majority of existing techniques only build Gabor feature vectors using the Gabor magnitude [40]. To get around this problem, a novel method of extracting these traits was reported in [39].

3.3 Features based on intrinsic mode functions

Getting the features from the Intrinsic Mode Function (IMF) is the goal of this stage. A data-dependent methodology known as Empirical Mode Decomposition (EMD) breaks down non-linear and stationary signals into symmetric parts known as intrinsic mode functions [42]. Two requirements must be satisfied by the IMF derived using the EMD technique. Firstly, there must be a minimum of one difference between the number of maximum and minimum minima. The second requirement is that the local maxima and local minima's mean values must equal or be less than zero. Sifting is an iterative procedure that may be used to extract the IMF from a signal ($s(t)$). The following steps are involved in the sifting process:

$$S(t) = \sum_{i=1}^{m} IMF_i(i) + R(t) \quad \text{(eq. 9)}$$

where "i" denotes residual, "r" denotes residual, and "M" is the number of extracted "IMF." For instance, the IMFs for one channel of data are displayed in Fig. 3, where "z" denotes the size of each signal and "t" is the time. The Sample signal for channel P7 and its IMFs are displayed in Fig. 3.

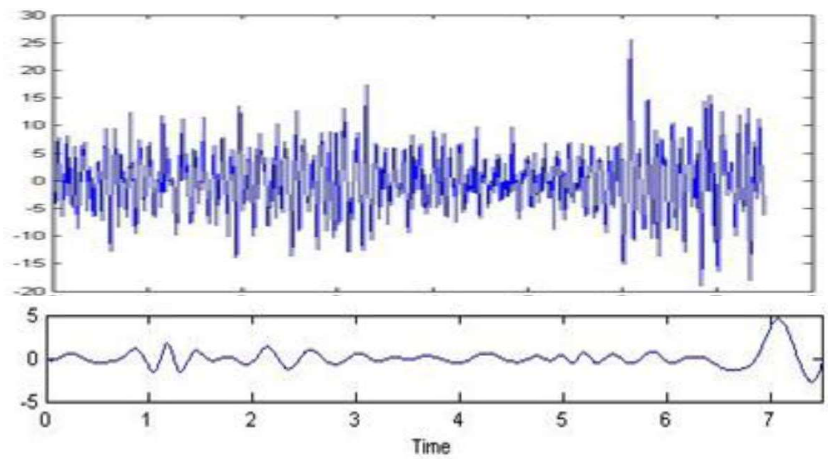

Figure 3. IMFs and Sample signal of channel P7

This work counts just three basic intrinsic mode functions for each signal and then takes the features out of these functions. Five characteristics are counted for each computed IMF: highest frequency center frequency root mean square variation of entropy The frequency at which 95% of the intrinsic mode function's energy is accessible in front of it is said to be the maximum frequency. The first and second IMF maximum frequencies are counted as characteristics of each channel in our analysis. For instance, count 14 items in our feature vector representing characteristics of the highest frequency of the IMF when there are 7 channels. The central frequency is the next characteristic, and IMFs are defined as the frequencies at which 50% of the energy of IMF signals is accessible. The fact that the EEG signals' entropy varies suggests that there has been a shift in how the brain functions. As a result, the entropy may occasionally represent information from the brain's cortex in addition to the statistical measure of the EEG pattern (10). The Shannon entropy is taken out of the IMFs in this study.

In general, the average power signal is the root mean square (RMS). In this study, the retrieved characteristics are the root mean square of the IMF. In this investigation, the root mean square was calculated using the first three IMFs. In statistics and probability theory, variance is the unit of dispersion. The characteristics from the IMF were extracted for this study using statistical data. Three IMF data are utilized to extract the features from each channel, much like with entropy and root mean square. The generation of feature vectors, maximum and center frequency, entropy, root mean square, and variance are the three characteristics that make up the variance for each channel. Two sets of features have been retrieved by us: The use of Gabor wavelet transformation on a picture is the subject of the first set of features. The collection includes phase features such as OGPCP and magnitude features such as mean and energy. Intrinsic mode functions yield the second set of characteristics.

3.4. Classification

In comparison to the previous techniques, this work has improved the accuracy of the input vector-based emotion recognition in this stage by utilizing a suitable classification algorithm. Finding a suitable classifier based on the obtained vector is the aim of this stage. A straightforward and incredibly accurate machine learning (ML) approach is SVM. The SVM seek to identify the best hyperplanes with the largest error margin. The genetic optimization approach is employed in this study to determine the ideal hyperplanes. This work has not employed optimal support vector machines in this phase since this work is aware of the emotions contained in the EEG signals. This work has a novel proposal for the classification stage which involves multidimensional SVM that has been tuned using a genetic algorithm, in addition to our innovations for the feature extraction step. Important parameters of SVM vary depending on the type of kernel function that is employed. Kernel functions translate data into other spaces with more dimensions where linear separation is possible, from the original space where it cannot be separated linearly.

In this work, the hyperplanes that are optimized are identified by the use of the genetic optimization technique. This work has not employed optimal support vector machines as had no idea about the emotions of EEG data. This work has a novel concept for the classification stage in addition to the innovations for the feature extraction step, which is the usage of multi-class SVM improved by genetic algorithm. Important parameters of SVM vary depending on the type of kernel function that is utilized in the SVM algorithms. Kernel functions translate information that is not linearly separable in the original space onto a greater dimensional space where it is. Several widely recognized kernel functions are presented, including the sigmoid, linear, and radial basis functions (RBF). This study makes use of the RBF. Two parameters, gamma, and c, must be specified to choose this function. The performance of the classifier is significantly impacted by these factors. Figure 4 illustrates how gamma and c affect classifier accuracy.

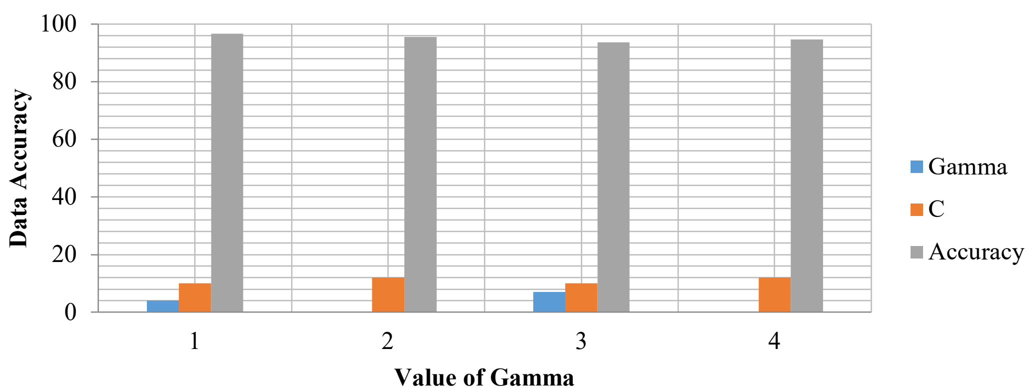

Figure 4. The effect of SVM parameters on classification accuracy

3.5 Cross Validation

The cross-validation method divides the training data into k sub-data sets. The unused sub-data set is utilized to assess performance, while the k-1 sub-datasets are used for training. Every k time that this procedure is carried out, a new subgroup is assessed. Every training set of data is only utilized once for assessment in this method. This work has used ten-fold cross-validation

4. Results and discussion

The Valence-Arousal model serves as the foundation for the emotion representation model used in this investigation. There are nine dimensions in all. This work has separated the VA space into 4 quadrants based on these assessments.
The EEG data is then labeled based on the valence and arousal ratings of the subjects. Four broad emotional states may be seen by splitting the Valence Arousal (VA) space into four quadrants: happy, sad, exciting, and hate. The EOG artifacts are eliminated together with a bandpass frequency filter 4.0–45.0 Hz preprocessing step on the original 128 Hz EEG data from the DEAP dataset. Thus, simply retrieved the specified.

4.1 Result of Channel distribution using S-Transformation and Gabar Method

The classifier will then be trained and tested using the complete dataset. For all experiments, a 10-fold cross-validation strategy is employed. With the help of a genetic method for optimizing the RBF kernel, the classifier—a multiclass SVM classifier—classifies the collected characteristics into four groups. The classification accuracy rate (CAR) serves as a gauge for the classifier's performance. The effect of two distinct sets of chosen EEG channel data on the emotion categorization accuracy (CAT) for four classes under consideration is depicted in Figure 5. Two Gabor filters are used in the tests. One filter is 5x9 and has 4 scales; the other is 5x10 and has 5 scales and 8 orientations. Two categories of channels exist: P7 channels, P3 channels, and PZ channels comprise the first group. The CP2 O1, C4, PO3, PZ, P3 and P7 channels make up the second group of channels.

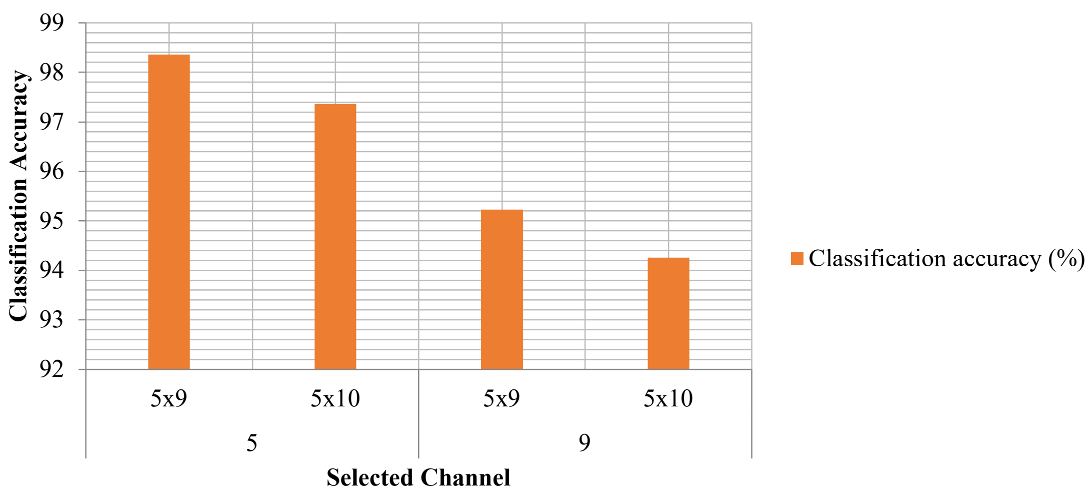

Figure 5: Impact of two distinct EEG channel signal selection groups on the accuracy of emotion categorization Accurate classification for two sets of channels with varying Gabor filter diameters A bigger feature vector is obtained by selecting more channels with longer Gabor filters. Table 4 illustrates that there is no direct correlation between the feature vector length and system performance. There are situations when the detection accuracy performs even worse when the feature vector length is increased. As a result, rather than the number of features, the efficiency of our system performance is directly correlated with the number of effective extracted features. Alternatively, a better processing speed can be achieved with a shorter feature vector.

This table demonstrates that an effective feature vector with higher classification accuracy may be generated by applying a Gabor filter with four scales and six orientations (5x9) and just three channels, P7, P3, and PZ. The length of the feature vector in this instance is 264. Certain characteristics need to be the same between various EEG emotion identification techniques to compare them. The input signal needs to be the same since the identification system receives different information from distinct data sets sampled at different frequencies.

Furthermore, different people respond to emotional stimuli at varying intensities. The total number of classes that need to be identical is the second argument. The suggested approach is contrasted with several recently released approaches in Figure 6. It is clear that the suggested approach greatly raises the EEG emotion detection accuracy. Only the procedure described under [2] was utilized as an input in the table below. This table was created using input from the DEAP dataset.

The procedure used is the same as that suggested in [2].

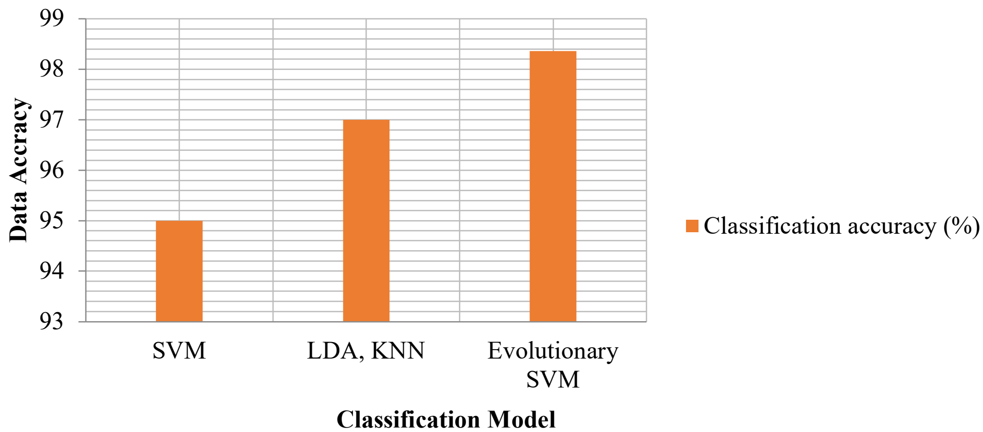

Figure 6: Comparison between the proposed method and pre-trained methods

As you can see, compared to previous algorithms, the suggested method performs better in emotion recognition. Furthermore, using the suggested technique, Figure 7 displays the confusion matrix for the four emotional states mentioned above.

Emotion	Happy	Sad	Current	Hate
Happy	98.36	0	1	1
Sad	4	94.32	1	0.68
Current	4	3	92	1
Hate	3	5	3	89.98
Accuracy	98.23	94.22	95.56	89.36

Figure 7: Proposed method Confusion matrix for identification of different emotional states

5. Conclusion

The objective of this research was to improve the accuracy of emotion recognisition system using EEG signals. This study utilzed the DEAP database for obtaining the different features. The data filteration was achived by Gabor filters using intrinsic mode functions. The feature extraction was done using S-Transformation extraction techniques. The performance of multiclass SVM classifier was found better as compared to other approaches which is further enhanced by the genetic evolutionary algorithm.The final result demonstrated a significant improvement in accuracy of 98.23% for emotion recognisition. The proposed system has successfully discriminated four distinct emotional states.

References

[1]. Pan J, Fang W, Zhang Z, Chen B, Zhang Z, Wang S. Multimodal emotion recognition based on facial expressions, speech, and EEG. IEEE Open Journal of Engineering in Medicine and Biology. 2023 Jan 27.

[2]. Chaudhari A, Bhatt C, Krishna A, Travieso-González CM. Facial emotion recognition with inter-modality-attention-transformer-based self-supervised learning. Electronics. 2023 Jan 5;12(2):288.

[3]. Sun Z, Zhang H, Bai J, Liu M, Hu Z. A discriminatively deep fusion approach with improved conditional GAN (im-cGAN) for facial expression recognition. Pattern Recognition. 2023 Mar 1;135:109157.

[4]. Marik A, Chattopadhyay S, Singh PK. A hybrid deep feature selection framework for emotion recognition from human speeches. Multimedia Tools and Applications. 2023 Mar;82(8):11461-87.

[5]. Niu W, Ma C, Sun X, Li M, Gao Z. A brain network analysis-based double way deep neural network for emotion recognition. IEEE Transactions on Neural Systems and Rehabilitation Engineering. 2023 Jan 12;31:917-25.

[6]. Asadzadeh S, Rezaii TY, Beheshti S, Meshgini S. Accurate emotion recognition utilizing extracted EEG sources as graph neural network nodes. Cognitive Computation. 2023 Jan;15(1):176-89.

[7]. Zhong MY, Yang QY, Liu Y, Zhen BY, Xie BB. EEG emotion recognition based on TQWT-features and hybrid convolutional recurrent neural network. Biomedical signal processing and control. 2023 Jan 1;79:104211.

[8]. Abdullah SM, Ameen SY, Sadeeq MA, Zeebaree S. Multimodal emotion recognition using deep learning. Journal of Applied Science and Technology Trends. 2021 May 30;2(01):73-9.

[9]. Sharma R, Pachori RB, Sircar P. Automated emotion recognition based on higher order statistics and deep learning algorithm. Biomedical Signal Processing and Control. 2020 Apr 1;58:101867.

[10]. Liu S, Gao P, Li Y, Fu W, Ding W. Multi-modal fusion network with complementarity and importance for emotion recognition. Information Sciences. 2023 Jan 1;619:679-94.

[11]. Iyer A, Das SS, Teotia R, Maheshwari S, Sharma RR. CNN and LSTM based ensemble learning for human emotion recognition using EEG recordings. Multimedia Tools and Applications. 2023 Feb;82(4):4883-96.

[12]. Prakash PR, Anuradha D, Iqbal J, Galety MG, Singh R, Neelakandan S. A novel convolutional neural network with gated recurrent unit for automated speech emotion recognition and classification. Journal of Control and Decision. 2023 Jan 2;10(1):54-63.

[13]. Sarvakar K, Senkamalavalli R, Raghavendra S, Kumar JS, Manjunath R, Jaiswal S. Facial emotion recognition using convolutional neural networks. Materials Today: Proceedings. 2023 Jan 1;80:3560-4.

[14]. Chowdary MK, Nguyen TN, Hemanth DJ. Deep learning-based facial emotion recognition for human–computer interaction applications. Neural Computing and Applications. 2023 Nov;35(32):23311-28.

[15]. Ramzan M, Dawn S. Fused CNN-LSTM deep learning emotion recognition model using electroencephalography signals. International Journal of Neuroscience. 2023 Jun 3;133(6):587-97.

[16]. Wang F, Wu S, Zhang W, Xu Z, Zhang Y, Wu C, Coleman S. Emotion recognition with convolutional neural network and EEG-based EFDMs. Neuropsychologia. 2020 Sep 1;146:107506.

[17]. Issa D, Demirci MF, Yazici A. Speech emotion recognition with deep convolutional neural networks. Biomedical Signal Processing and Control. 2020 May 1;59:101894.

[18]. Mellouk W, Handouzi W. Facial emotion recognition using deep learning: review and insights. Procedia Computer Science. 2020 Jan 1;175:689-94.

[19]. Petrantonakis PC and Hadjileontiadis LJ. “Emotion recognition from EEG using higher order crossings” IEEE Trans. on Information Technology in Biomedicine, vol. 14, no.2, pp.186–197, 2010, doi: 10.1109/TITB.2009.2034649.

[20]. Petrantonakis PC and Hadjileontiadis LJ. “A novel emotion elicitation index using frontal brain asymmetry for enhanced EEG based emotion recognition” IEEE Trans. on Information Technology of Biomedical, vol. 15, no.5, pp. 737-46, 2011, doi: 10.1109/TITB.2011.2157933.

[21]. Hosseini S, Khalilzadeh M, Naghibi-Sistani M and Niazmand V. ” Higher Order Spectra Analysis of EEG Signals in Emotional Stress States” IEEE International Conf. on Information Technology and Computer Science, pp. 60–63, 2010, doi: 10.1109/ITCS.2010.21.

[22]. Nie D, Wang XW, Shi LC and Lu BL. “EEG-based Emotion Recognition during Watching Movies” IEEE International Conf. on Neural Engineering, pp.667–670, 2011.

[23]. Liu Y and Sourina O. “EEG-based dominance level recognition for emotion-enabled interaction” IEEE International Conf. on Multimedia and Expo., pp.1039–1044, 2012, doi: 10.1109/ICME.2012.20

[24]. Reuderink B, Muh C and Poel M. “Valence, arousal and dominance in the EEG during game play”, International Journal of Autonomous and Adaptive Communications Systems, vol. 6, no. 1, pp. 45–62, 2013, doi: 10.1504/IJAACS.2013.050691.

[25]. Rozgi´c V, Vitaladevuni S and Prasad R. “Robust EEG emotion classification using segment level decision fusion” International Conf. on Acoustics, Sound and Signal Processing (ICASSP), pp.1286–1290, 2013.

[26]. [23] Soleymani M, Kolestra S, Patras I and Pun T. “Continuous emotion detection in response to music videos” IEEE International Conf. on Automatic Face & Gesture Recognition, pp.803–808, 2011.

[27]. Stelios K and Hadjidimitriou LJ. “Toward an EEG-based recognition of music liking using time-frequency analysis” IEEE Trans. on Biomedical Engineering, vol. 59, no. 12, pp.3498–3510, 2012, doi: 10.1109/TBME.2012.2217495.

[28]. Murugappan M, Nagarajan R and Yaacob S. “Classification of human emotion from EEG using discrete wavelet transform” Journal of Biomedical Science and Engineering, vol.3, no.4, pp. 390–396, 2010, doi: 10.4236/jbise.2010.34054.

[29]. Hadjidimitriou SK and Hadjileontiadis LJ. “Toward an EEG-based recognition of music liking using time-frequency analysis” IEEE Trans. on Biomedical Engineering, vol. 59, no.12, pp.3498–510, 2012, doi: 0.1109/TBME.2012.2217495.

[30]. Bajaj V and Pachori RB. “Detection of Human Emotions Using Features Based on the Multiwavelet Transform of EEG Signals”, In: Hassanien (editor): Brain-Computer Interfaces. Springer International Publishing. Switzerland. pp. 215-240, 2015, doi: 10.1007/978-3-319-10978-7_8.